ELSEVIER

Coordination Chemistry Reviews
178–180 (1998) 723–753

COORDINATION CHEMISTRY REVIEWS

Rare earth metal borocarbides Examples of coordination compounds in solid-state chemistry[1]

Josef Bauer, Jean-François Halet *, Jean-Yves Saillard *,[2]

Laboratoire de Chimie du Solide et Inorganique Moléculaire, UMR 6511 Université de Rennes 1, Avenue du Général Leclerc, 35042 Rennes, Cedex, France

Received 12 December 1997; accepted 25 March 1998

Contents

Abstract

A variety of structural types of solid-state rare earth metal borocarbide materials containing infinite two-dimensional layers, infinite one-dimensional chains, or finite groups of boron and carbon are reviewed. Although the solid-state language of Zintl–Klemm concept, band structures, and density of states is necessary to rationalize this kind of compound, they are governed by the laws that guide most molecular and solid-state structural chemistry: the relationship between the electron count and the structural arrangement. More precisely, one could think

* Corresponding author. Fax: +33 2 99 63 57 04; e-mail: halet@univ-rennes1.fr
[1] Dedicated to Professor Roald Hoffmann on the occasion of his 60th birthday.
[2] Also corresponding author; saillard@univ-rennes1.fr

PII S0010-8545(98)00106-4

of these materials as solid-state coordination compounds in which the classical bonding scheme of σ-donation, sometimes supplemented by some π-backdonation, is present.

Keywords: borocarbide; coordination chemistry; electronic structure; rare earth metal; solid-state structure

1. Introduction

The structural chemistry of boron-containing compounds is particularly rich and varied (see for instance refs. [1–4]). It includes ternary rare earth metal borocarbide solid-state materials of formula $M_xB_yC_z$ (M = Sc, Y, Ln, An), which constitute a growing family offering a broad diversity of original topologies, most of them unique, especially with respect to the bonding within the non-metal frameworks. [Throughout this review, the words "rare earth metal" refer to the elements Sc, Y, lanthanides and actinides.] These compounds, generally prepared by arc melting techniques, receive increasing attention these days because of their mechanical, magnetic and electrical properties. As far as we know, all are electrical conducting materials and some of them have even demonstrated superconducting behavior at low temperature. Those having been structurally characterized are listed in Table 1. They can be classified into three categories, depending upon the arrangement of the non-metal atoms. In the first category, boron and carbon atoms form infinite, planar, two-dimensional (2-D) networks which alternate in the solid with 2-D sheets of metal atoms. In the second family, the association of boron and carbon gives rise to infinite one-dimensional (1-D) zig-zag chains of boron atoms on which carbon atoms are tethered. These branched chains, isolated from each other, are inserted in channels built by the metal atoms. The third category contains compounds in which boron and carbon atoms assemble to linear or quasi-linear finite pseudo-molecules trapped into holes made by the metallic matrix. These finite chains can have different sizes, ranging hitherto from three atoms, such as BC_2 in Sc_2BC_2 [20] for instance, to 13 atoms, such as B_5C_8 in $C_{10}B_9C_{12}$ [17]. Note that in the same material chains of different size, as well as isolated C atoms or C_2 units, can co-exist (see Table 1).

According to electronegativities, charge transfer must proceed from the rare earth metals to boron and carbon. Using the Zintl–Klemm concept [22,23], that is assuming an ionic bonding mode between fully oxidized metal atoms (usually M^{3+}, sometimes M^{4+} such as Ce or Th) and the anionic B/C system, it is possible to define an averaged valence electron count (VEC) per non-metal atom. For a compound of general formula $M_xB_yC_z$, $VEC = (nx + 3y + 4z)/(y + z)$, with $n = 3$ or 4 depending on the metal oxidation state [24]. The VEC values have been calculated for the compounds given in Table 1. They should be considered as only approximate values since, even considering the ionic bonding scheme as satisfactory, the metal atoms do not always need to be fully oxidized to fulfil the electronic requirements of the anionic boron–carbon entities (vide infra). Nevertheless, such an approach

Table 1
Different $M_xB_yC_z$ rare earth metal borocarbides structurally characterized. The VEC is calculated with $n=3$. It is given in brackets for $n=4$

Structural type		VEC[a]		B–C network	$(y+z)/x$	Reference
Two-dimensional networks						
LaB_2C_2	(Y to Lu)	4.25		$2/_\infty$-(2B2C).(4B4C)	4.0	[5]
ScB_2C_2		4.25		$2/_\infty$-(2B3C).(4B3C)	4.0	[6]
YB_2C	(Sc, Tb to Lu)	4.33		$2/_\infty$-(2B2C).(5B2C)	3.0	[7,8]
ThB_2C	(Ce, U[b], Np, Pu)	4.33	(4.67)	$2/_\infty$-(6B).(6B(3C))	3.0	[9]
UB_2C[c]		4.33	(4.67)	$2/_\infty$-(6B(2C))	3.0	[10]
$Gd_2B_3C_2$		4.60		$2/_\infty$-(8B4C)	2.5	[11]
Infinite branched chains						
YBC	(Dy, Ho, Er)	5.00		$1/_\infty$-$[B_2C_2]$	2.0	[7,8]
ThBC		5.00	(5.50)	$1/_\infty$-$[B_2C_2]$	2.0	[12]
UBC	(Np, Pu)	5.00	(5.50)	$1/_\infty$-$[B_2C_2]$	2.0	[13]
$UB_{0.78}C_{1.22}$		5.11	(5.61)	$1/_\infty$-$[B_2C_2]$	2.0	[14]
$Th_3B_2C_3$		5.40	(6.00)	[C]-$1/_\infty$-$[B_2C_2]$	1.67	[15]
Finite linear chains						
$La_{15}B_{14}C_{19}$		4.94		$[B_4C_7][B_5C_6]$	2.2	[16]
$Ce_{10}B_9C_{12}$	(La, Nd)	5.00		$[B_5C_8][B_4C_4]$	2.1	[17]
$Ce_5B_4C_5$		5.22		$[B_4C_4][B_3C_3][BC_2][C]$	1.8	[18]
$Ce_5B_2C_6$	(La, Gd, Ho)	5.63		$[BC_2][C_2]$	1.6	[19]
Sc_2BC_2		5.67		$[BC_2]$	1.5	[20]
$Gd_5B_2C_5$	(Sm)	5.86		$[BC_2][C]$	1.4	[21]

[a] Averaged valence electron count per main group atom.
[b] High temperature.
[c] Low temperature.

provides a crude relationship between the number of electrons and the dimensionality of the non-metal network present in these compounds. Phases with 2-D boron–carbon networks are associated with the lowest VECs, whereas the largest VECs are found for the phases containing finite linear boron–carbon chains. The materials containing 1-D non-metal networks are characterized by intermediate VEC values. This trend can be explained by the fact that, for a given stable compound, formal adding of supplementary electrons will result in the occupation of antibonding B/C levels. Consequently, bond breaking is expected, inducing a decrease in the connectivity between the atoms and thus the dimensionality of the non-metal network.

Although it provides a rough rationalization of the $M_xB_yC_z$ phases, the calculation of VEC is not sufficient to understand the local environment of the boron and carbon atoms. A deeper insight into the rationalization of this extremely rich structural chemistry can be obtained through an overview of the various theoretical analyses which have been carried out on these compounds, particularly in our laboratory [11,20,24–29]. Therefore, this review deals not only with the description and classification of the crystal structures of rare earth metal borocarbides, but also with their bonding and rationalization. A somewhat personal evaluation is presented

from a molecular viewpoint regarding these solid-state compounds as giant "metal complexes". Emphasis is placed on the "coordination" aspect encountered in this kind of solid-state material.

Hitherto, the majority of theoretical work devoted to this kind of compound has been within the one-electron non-self-consistent extended Hückel tight-binding (EHTB) method [30–33], sometimes complemented by quantitative self-consistent ab initio Hartree–Fock (HF) or density functional theory (DFT) methods (for an introduction to density functional theory, see for instance refs. [34–36]). From the results obtained, it appears that the bonding between the light atoms can be understood assuming in a first approximation a purely ionic bonding mode between the metallic cations and the anionic boron–carbon sublattice. This is a crude approximation. Indeed, a large degree of covalent metal–non-metal bonding is present in these phases. Nevertheless, it allows in most cases a complete understanding of the topology of the non-metal networks. Therefore, the first and crucial question when looking at the bonding in a particular $M_xB_yC_z$ compound is that of the metal oxidation state, i.e. how many metal electrons need formally to be transfered to satisfy the electronic demands of the boron–carbon entities. An answer is provided in the following sections for the different families of rare earth metal borocarbide phases given in Table 1.

2. Two-dimensional boron–carbon networks

Layered compounds made of alternate boron–carbon and metallic sheets constitute a substantial class among the M–B–C materials. They are generally characterized by a VEC around 4–4.5.

2.1. The MB_2C_2 phases

Two different MB_2C_2 structural types have been characterized, namely LaB_2C_2 [5] and ScB_2C_2 [6]. They are shown in Fig. 1. The LaB_2C_2 type exists for the whole lanthanide series as well as for Y and Ca [2]. A recent investigation into YB_2C_2 indicates that these phases adopt a tetragonal layered structure [see Fig. 1(a)] [37]. Within the boron–carbon 2-D layer, each atom is bonded to three other atoms so as to form fused four- and eight-membered rings. Each four-membered ring is made of two boron and two carbon atoms in opposite positions, whereas each eight-membered ring contains four boron and four carbon atoms with B–B, B–C and C–C contacts (1.64, 1.61, and 1.37 Å, respectively in YB_2C_2) [37]. In ScB_2C_2, the boron–carbon layers consist of fused five- and seven-membered rings [see Fig. 1(b)]. The metal atoms are located above and below the eight-membered rings, in LaB_2C_2 type phases, above and below the seven-membered rings in the ScB_2C_2 phase.

In both 2-D boron–carbon networks, all the atoms are three-connected. Indeed, these two planar arrangements of sp^2-type atoms are isostructural to hypothetical metastable allotropic forms of carbon which have been proposed by Balaban et al. [38,39]. This suggests a formal charge partitioning $(M^{2+})(B_2C_2)^{2-}$. Consequently,

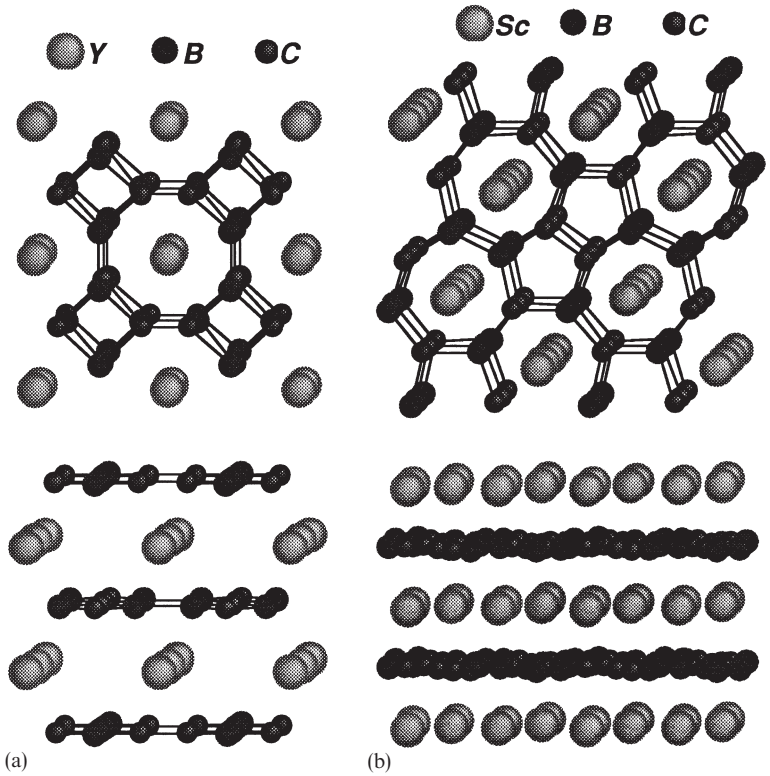

Fig. 1. Top view and side view of the structural arrangement of (a) YB_2C_2 and (b) ScB_2C_2.

both $(B_2C_2)^{2-}$ networks present in LaB_2C_2 and ScB_2C_2 type phases can be described by several canonical Lewis formulae in which all the atoms satisfy the octet rule.

It turns out that the distribution of the non-metallic atoms in the B–C networks associated with this formal charge partitioning, frequently termed the "coloring problem" [40], has been widely debated in the literature and is still controversial [41]. Smith et al. initially proposed a coloring with alternating boron and carbon atoms for the MB_2C_2 (M = lanthanide) compounds [42]. Among several possible canonical formulae for such a coloring, two of them are shown in **1**. Some years later, the alternative pattern shown with two possible Lewis formulae in **2** was initially proposed by Bauer et al. for YB_2C_2, LaB_2C_2, and CaB_2C_2, and recently confirmed for YB_2C_2 on the basis of X-ray measurements [5,7,8,37]. EHTB calculations by Burdett et al. on these two possible structures found that coloring **1** is the most energetically stable for an isolated $(B_2C_2)^{2-}$ 2-D system [41]. Indeed, the comparison of the density of states (DOS) of the 2-D $(B_2C_2)^{2-}$ nets **1** and **2** indicates that the latter, for which there is no gap at the Fermi level (i.e. no HOMO/LUMO gap), is unstable with respect to the former, for which a significant band gap is opened at the Fermi level. A molecular analogy can be made with the square

cyclobutadiene molecules which are best stabilized by attaching electron-donating and electron-withdrawing groups alternately around the ring and $B_2X_2R_2$ (X = N, P) molecules (see for example ref. [43]).

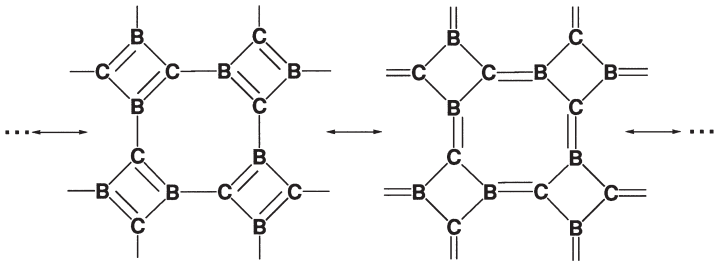

(1)

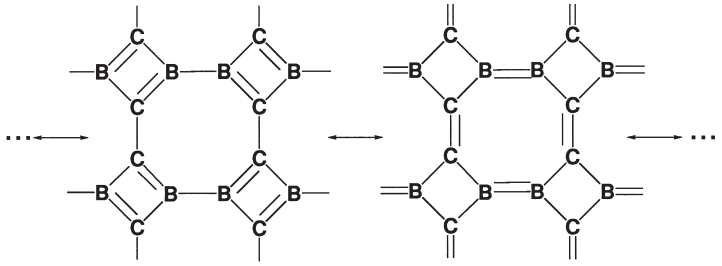

(2)

Calculations on the full 3-D CaB_2C_2 and LaB_2C_2 compounds confirm the energetic preference for isomer **1**, suggesting that the La atoms act as two-electron donors to the boron–carbon sheets, the third valence electron remaining in the narrow d metallic band [41]. On the other hand, the same authors found the opposite coloring **2** to be the most stable in the case of a $(B_2C_2)^{4-}$ 2-D system, but gave no indication on the $(B_2C_2)^{3-}$ case. Therefore, the question of the metal oxidation state in the case of M = Y or lanthanide remains open. Indeed, an accurate single-crystal X-ray study carried out recently by Pöttgen [37] and ^{11}B NMR measurements performed by Le Floch et al. [44] found coloring **1** to be that of YB_2C_2 [see Fig. 1(a)]. These new results suggest that, contrary to the EHTB calculations on the 3-D LaB_2C_2 structure, the metal-to-non-metal electron transfer is complete in the case of M = rare earth metal.

The different arrangement in the non-metallic planes observed for ScB_2C_2 [see Fig. 1(b)] is often interpreted as resulting from the smaller size of Sc compared to Y and the lanthanides [6]. However, Burdett et al. have proposed an electronic explanation [40] based on the oxidation states of the metal atoms. According to these authors, ScB_2C_2 should be best described with the $(Sc^{3+})(B_2C_2)^{3-}$ charge partitioning, while they propose $(M^{2+})(B_2C_2)^{2-}$ for the LaB_2C_2 structure type (see

above). Obviously, more experimental and theoretical data on the various MB_2C_2 compounds are needed to clarify the bonding in these phases.

An alternative arrangement has been reported for MgB_2C_2 [45]. According to $(Mg^{2+})(B_2C_2)^{2-}$, this material contains graphite-like sheets slightly puckered because of the specific distribution of the metal atoms above and below. This arrangement, isoelectronic with that noticed in CaB_2C_2, has not been observed yet with rare earth metals.

2.2. The MB_2C phases

The three structural types which have been reported for the MB_2C phases, namely ThB_2C [9], α-UB_2C [10], and YB_2C [7,8], are shown in Fig. 2. Although they all present similar packing of alternating metal and non-metal layers, they differ significantly from their topologies within the boron and carbon networks. In ThB_2C boron hexagons are fused with nine-membered rings of boron and carbon atoms. The α-UB_2C phase presents fused eight-membered rings of light atoms, whereas fused four- and seven-membered rings are encountered in YB_2C.

In fact, ThB_2C and α-UB_2C are strongly related both from the structural and electronic viewpoint. As can be seen in **3** and **4**, the 2-D arrangement of the non-metallic network in both compounds is made of the same linear $B(sp^2)$–$C(sp)$–$B(sp^2)$ building blocks. The B–C–B units assemble together through $B(sp^2)$–$B(sp^2)$ single-bond contacts (ca. 1.8 Å). In ThB_2C, the arrangement of the boron atoms in hexagons is structurally reminiscent of that observed in benzene. The 2-D non-metal network of α-UB_2C can be described as a set of infinite chains of sp^2 boron atoms resembling the ideal *cis–trans* conformation of polyacetylene, linked to each other. The rather short B–C distances (ca. 1.5 Å) suggest some B–C double-bond character [24]. Double bonds would be nicely accounted for with the formal $(M^{2+})(B_2C)^{2-}$ charge partitioning. However, such a formal charge is not consistent with the two sp^2 boron atoms being coplanar. Indeed, a 16-electron $(B_2C)^{2-}$ repeat unit is isoelectronic with allene, $H_2C{=}C{=}CH_2$, and consequently is expected to adopt the non-planar geometry **5** instead, in which the boron coordination planes are perpendicular to each other. This is supported by ab initio calculations on the isoelectronic molecular model $[H_2B{=}C{=}BH_2]^{2-}$, which was found to adopt the same non-planar D_{2d} symmetry as allene [25]. It is possible in turn to imagine an MB_2C structure based on the assembly of allenic-like $(B_2C)^{2-}$ segments. As shown in Fig. 3, a 3-D boron–carbon arrangement is obtained with holes in which would reside the divalent metal atoms such as, for instance, Mg^{2+}. Another way to look at the B–C network of this hypothetical structure is to consider layers of isolated infinite zig-zag boron chains running perpendicular to each other, linked by carbon atoms. It turns out that this B–C arrangement mentioned here is identical to one of the numerous hypothetical allotropic forms recently proposed by Elguero et al. [46]. Preliminary EHTB and DFT calculations on these arrangements suggest that this type of material should be metallic, if it exists [47].

A better formal charge which would account for the co-planarity of the sp^2 boron atoms in the B–C–B repeat unit present in ThB_2C and α-UB_2C is 4−, as exemplified

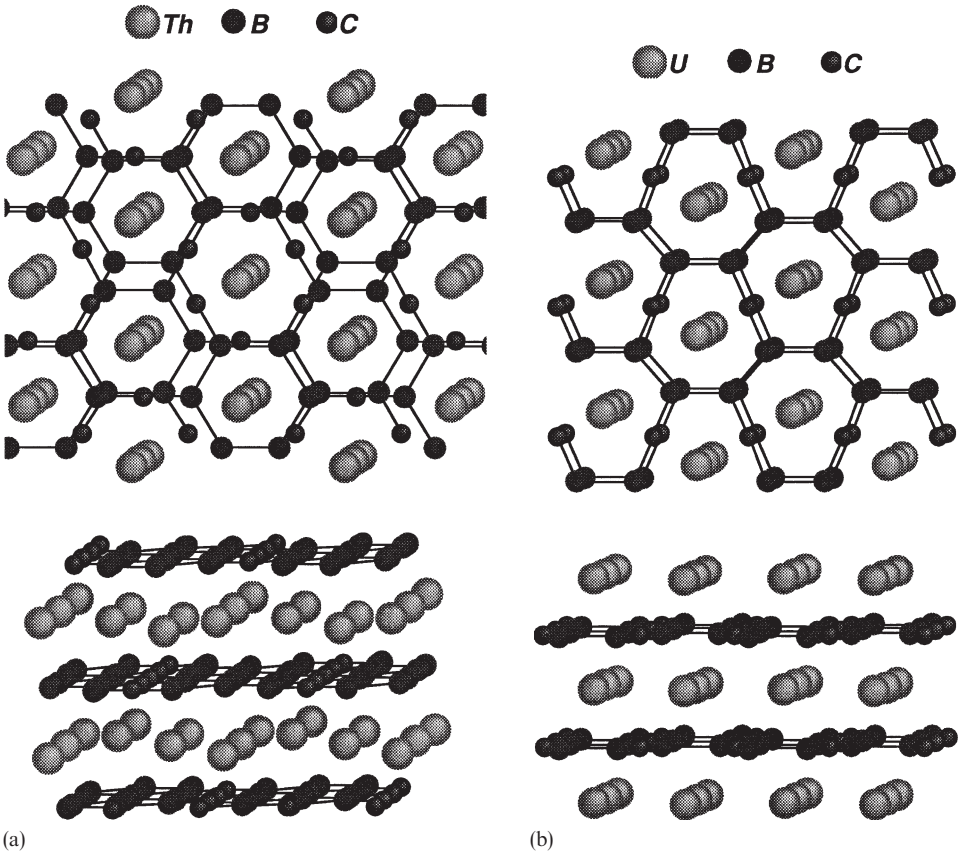

Fig. 2. Top view and side view of the structural arrangement of (a) ThB_2C, (b) α-UB_2C, and (c) Sc B_2C_2.

by the canonical formulae shown in **6**, in which all the atoms satisfy the octet rule. The possibility of an oxidation state of 4+ for Th and U allows such a charge distribution. The $(B_2C)^{4-}$ building block possesses four π-electrons with a B–C bond order of 1.5. It allows the 2-D boron–carbon network to be planar. However, a new question arises: why is the sp carbon atom linearly coordinated? A bent (BCB) angle with an sp^2 carbon atom is intuitively expected from **6**. It turns out that EH and ab initio calculations show that the answer lies in the electronegativity difference between boron and carbon [24,25]. Calculations on several isoelectronic molecular models, such as $[H_2CCCH_2]^{2-}$, $[H_2BCBH_2]^{4-}$ or $[H_2BOBH_2]^{2-}$, indicate that the optimized (CCC) angle is, as expected, close to 120° in the former. On the other hand, the potential energy surface associated with the bending is flat around linearity in the other two models containing atoms with different electronegativities. This opposition to bending due to an electronegativity effect should be general in chemistry.

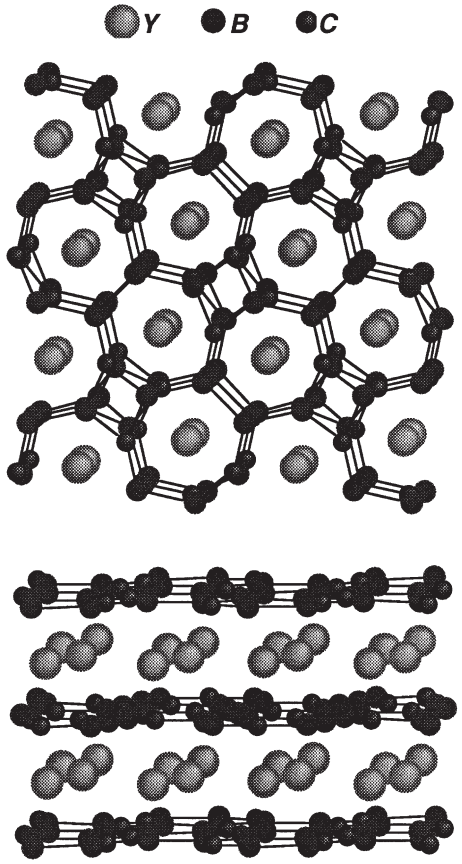

(c)

Fig. 2. (*continued*)

EHTB calculations on the 2-D $(B_2C)^{4-}$ nets present in ThB_2C and α-UB_2C give comparable results [24]. Their total energies differ by only 0.06 eV per B_2C repeat unit, a value which is not significantly different from zero at the considered level of theory. In both cases, the computed number of π-electrons per $(B_2C)^{4-}$ unit is exactly or almost exactly equal to 4, in full agreement with the Lewis structures drawn in **6**. The DOS of these 2-D sublattices are very similar, exhibiting a semimetallic shape for the considered electron count. This is exemplified in Fig. 4(a) which shows the DOS of the $(B_2C)^{4-}$ net of α-UB_2C. As we will see later, this semimetallic feature is a characteristic of the non-metal anionic networks of many rare earth metal borocarbides. Another common characteristic is the shape of the B–B crystal orbital overlap population (COOP) curve [24]. This curve, which shows the variation of the average B–B overlap population with respect to energy, is given in Fig. 4(b) in the case of the $(B_2C)^{4-}$ net of α-UB_2C. It is positive below the Fermi

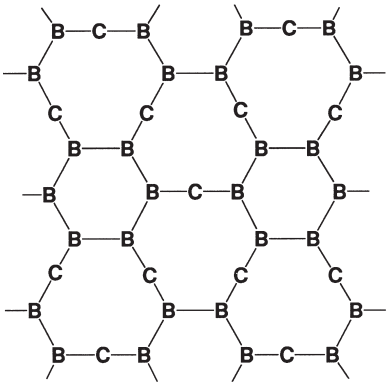

(3)

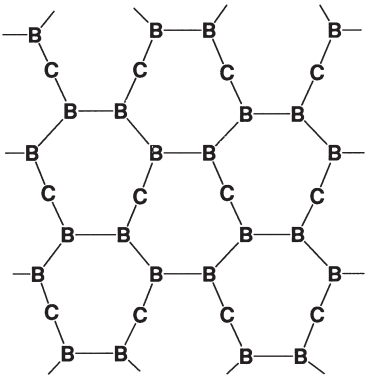

(4)

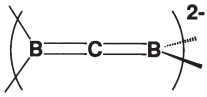

(5)

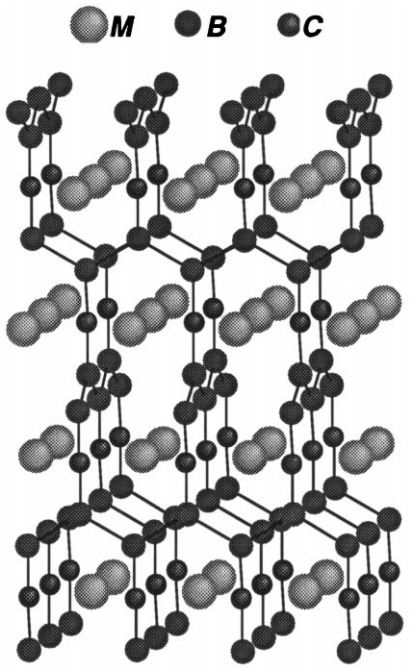

Fig. 3. Hypothetical arrangement for MB_2C based on the assembly of allenic-like $(BC_2)^{2-}$ units.

(6)

level, and changes its sign right at the Fermi level to become negative above the Fermi level. This is not the case for the B–C overlap population [see Fig. 4(b)], which changes its sign far below the Fermi level. Therefore, B–B bonding in these $(B_2C)^{4-}$ planes is optimum, while B–C bonding is not. This result suggests that the topology of the non-metallic systems in these phases is dominated by the B–B bonding interactions.

As for the isolated non-metallic sublattices, EHTB calculations carried out on the full 3-D ThB_2C and α-UB_2C materials give very similar results [24]. The total DOS and the metal projection of α-UB_2C are shown in Fig. 4(c). The levels situated above the Fermi level are mainly metallic in character. The presence of this d-band above the Fermi level is in full agreement with an oxidized tetravalent metal. The states situated below the Fermi level derive mainly from the occupied states of the isolated $(B_2C)^{4-}$ 2-D fragments. However, they present some significant metal character, indicating a rather strong covalent interaction between occupied orbitals of the $(B_2C)^{4-}$ network and the vacant metal d orbitals. A transfer of approximately one π-electron per formula unit occurs from $(B_2C)^{4-}$ into the 6d metal orbitals in both MB_2C (M = Th, U) phases. This illustrates that a purely ionic picture is a good starting point to explain the arrangement observed in the different non-metal networks, but not sufficient to describe the total bonding mode in these types of compounds.

The structure and electronic properties of ThB_2C and α-UB_2C are closely related. At high temperature the α-UB_2C phase transforms into the β-UB_2C phase, which is isostructural to the ThB_2C arrangement. A concerted mechanism for the transformation has been proposed [10]. A theoretical investigation of this mechanism suggests that the empty 6d metallic band might act as an electron buffer during the transformation process, first accepting electrons from the non-metal lattice and then releasing them [24].

The reason why the topology of the non-metal sublattice in YB_2C is not directly related to that of ThB_2C and α-UB_2C (see Fig. 2) comes from the different oxidation states of the metal atoms. In the former case, the metal cannot be tetravalent and the best formal charge partitioning is $(Y^{3+})(B_2C)^{3-}$ [24]. For this electron count, four canonical Lewis structures, all satisfying the octet rule for B and C, account for the planarity and the partial double-bond character of the B–C bonds. One of them is shown in **7**. It is noteworthy that such a description corresponds also to four π-electrons per $(B_2C)^{3-}$ repeat unit, as for the $(B_2C)^{4-}$ repeat units in the ThB_2C and α-UB_2C systems. The total charges of the B_2C building blocks being different, they differ by the number of σ-electrons, which is lower by one in the

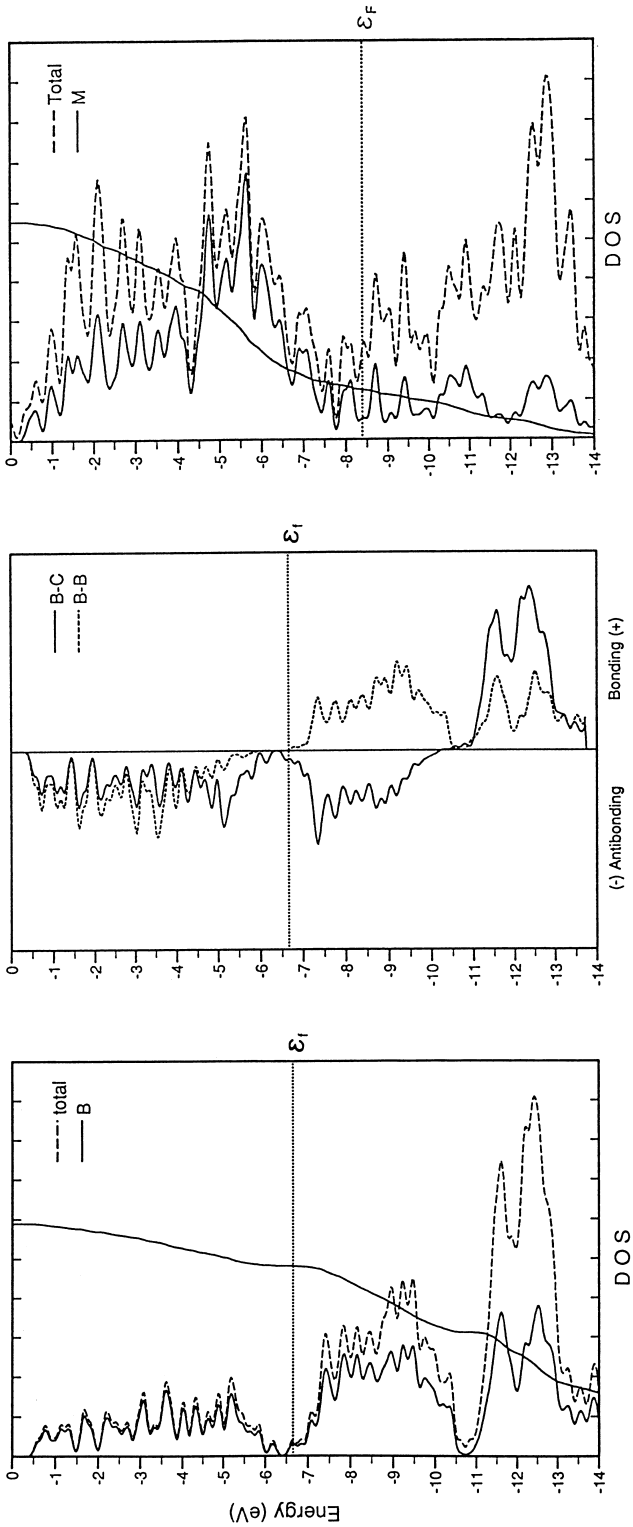

Fig. 4. (a) Total density of states (dashed line) and boron contribution (solid line). (b) COOP curves for B–B (solid line) and B–C (dashed line) contacts for the 2-D boron–carbon net $(B_2C)^{4-}$ present in α-UB_2C. (c) Total density of states (dashed line) and metal contribution (solid line) of α-UB_2C.

YB_2C phase. As a consequence, the number of σ bonds is larger in YB_2C, the carbon now being triconnected. Nevertheless, the DOS and COOP curves of the 2-D $(B_2C)^{3-}$ net present in YB_2C are strongly related to the corresponding curves of the $(B_2C)^{4-}$ of α-UB_2C for instance (compare Figs. 4 and 5). In particular, a semi-metallic character at the Fermi level in the DOS and the change of sign of the B–B overlap population at the Fermi level are also noticed (experimental B–B separations are comparable to those measured in ThB_2C and α-UB_2C [7–10]). The computed number of π-electrons per $(B_2C)^{3-}$ unit is almost exactly equal to four, in agreement with several canonical formulae such as that shown in **7**. These similarities originate mainly from the π-electronic structures of the non-metal anionic networks, which are strongly related in the three MB_2C phases. As a consequence, their covalent bonding with the metal sublattice is also related. The EHTB total DOS and metal projection of YB_2C look similar to those of the other MB_2C phases, and the π-electron transfer from the $(B_2C)^{3-}$ repeat segments into the 3d AO of the Y^{3+} cations is also close to one [24].

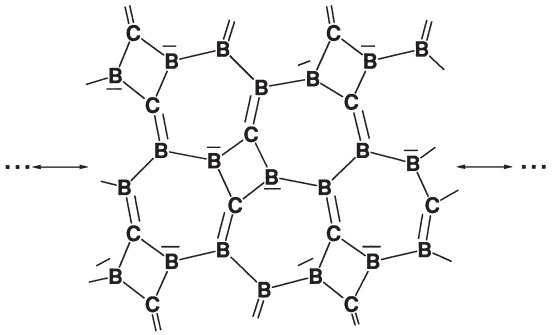

(7)

2.3. *The $Gd_2B_3C_2$ phase*

We have seen in **3** and **4** two ways to construct 2-D nets from the assembly of linear and planar $(B_2C)^{4-}$ segments. An alternative arrangement consists of infinite zig-zag chains of boron atoms, resembling the all-*trans* conformation of polyacetylene, linked to each other via sp carbon atoms, as depicted in **8**. EHTB calculations on such a hypothetical $(B_2C)^{4-}$ 2-D framework give no significant differences with the results obtained for the isoelectronic 2-D systems mentioned previously [24]. Therefore, such a non-metal network should be stable as part of a metal ternary or quaternary phase, providing that there is space enough for inserting the cations.

It turns out that the presence of such zig-zag chains of boron atoms inserted in a 2-D boron–carbon net is observed in the $Gd_2B_3C_2$ phase, as shown in Fig. 6. In this compound, the building block of non-metallic planes is not the simple B–C–B motif as in ThB_2C and UB_2C, but rather a longer B–C–B–C–B linear unit [11]. The B–B distances are 1.92 Å, whereas the B–C distances are either 1.41 Å or 1.60 Å. EH

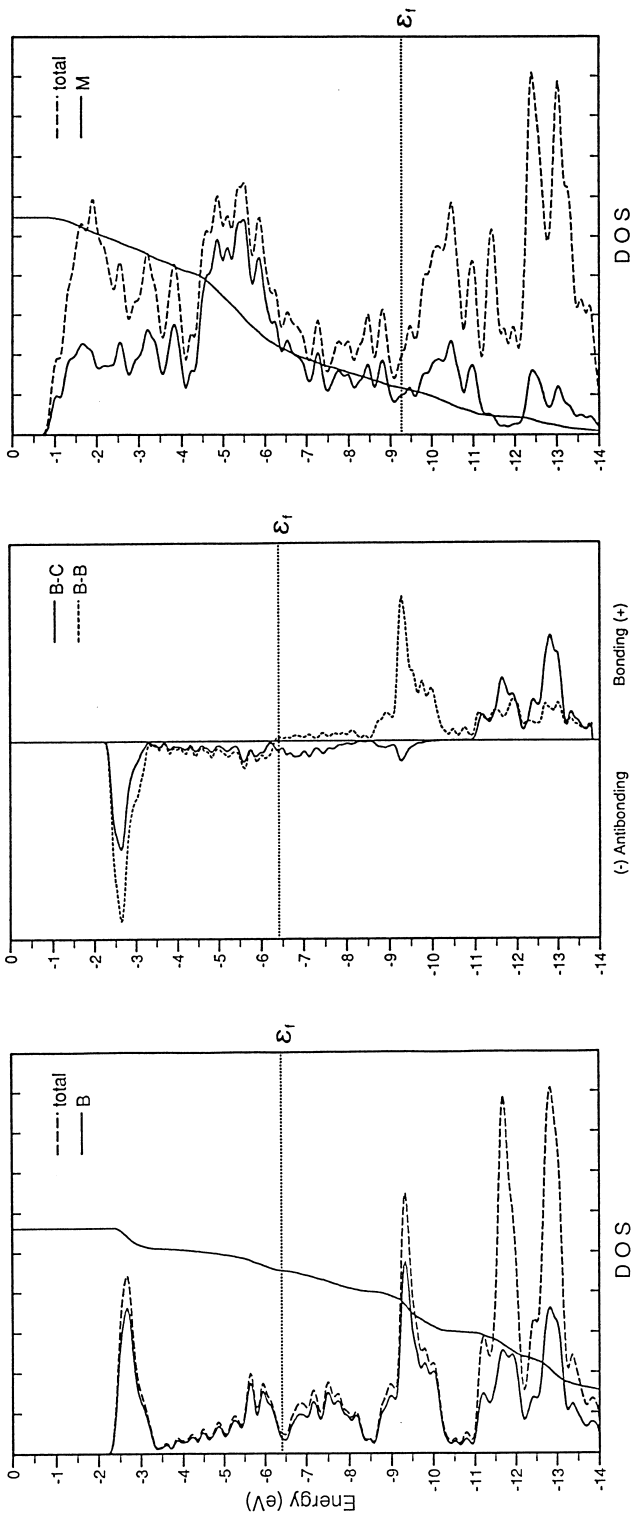

Fig. 5. (a) Total density of states (dashed line) and boron contribution (solid line). (b) COOP curves for B–B (solid line) and B–C (dashed line) contacts for the 2-D boron–carbon net $(B_2C)^{3-}$ present in YB_2C. (c) Total density of states (dashed line) and metal contribution (solid line) of YB_2C.

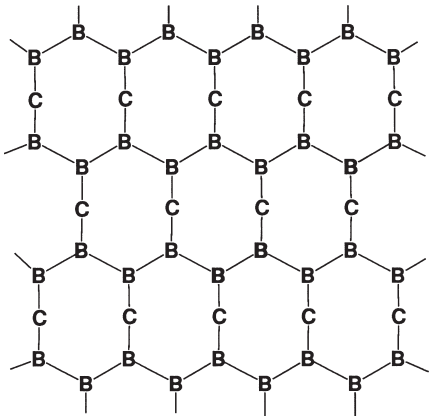

(8)

and ab initio calculations on various anions of the $H_2BCBCBH_2$ molecular model indicate that the best formal charge for this 2-D network is $(B_3C_2)^{5-}$. This charge corresponds to the canonical formulae **9** in which all the atoms obey the octet rule. Such an electron distribution accounts nicely for the planarity of the network, as well as the linearity of the B_3C_2 motif, which is also related to the electronegativity difference between carbon and boron. EHTB calculations on the $(B_3C_2)^{5-}$ 2-D sheet present in $Gd_2B_3C_2$ lead to similar electronic characteristics for the DOS and B–B overlap population as those described above for the non-metal anionic B_2C sublattices. The assignment of the formal charge of 5− to the non-metal repeat unit leads to a mean oxidation state of 2.5+ for Gd. In other words, the metal atoms do not need to be fully oxidized to fulfil the electronic demands of the B–C framework. Consistently, the DOS of the full 3-D $Gd_2B_3C_2$ generates in the bands around the Fermi level a metal character slightly larger than that in the MB_2C phases [11].

(9)

3. Infinite boron–carbon chains

The three structural types corresponding to the MBC stoichiometry, YBC [7,8], UBC [13], and ThBC [12], are illustrated in Fig. 7. In all of them, the metal atoms depict trigonal prisms which condense along one direction through square faces and along another direction through triangular faces, forming infinite 2-D slabs. Boron

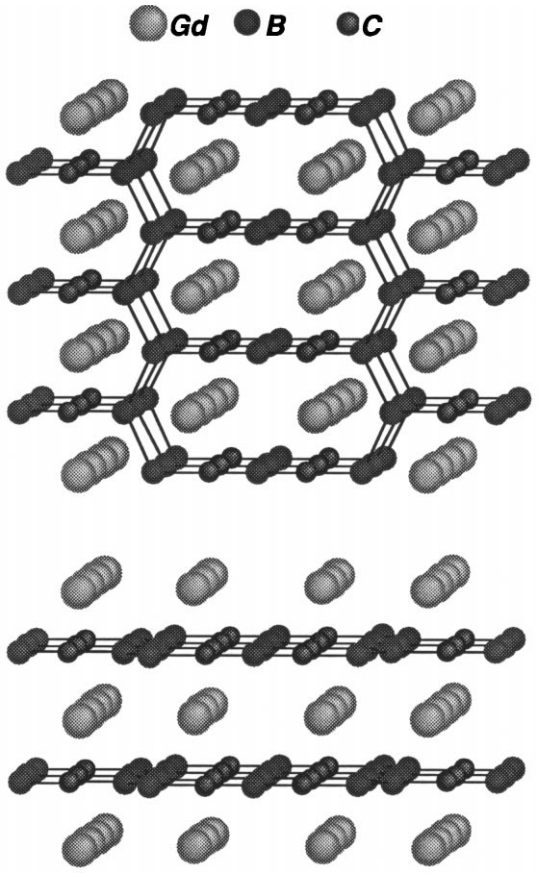

Fig. 6. Top view and side view of the structural arrangement of $Gd_2B_3C_2$.

atoms are located at the center of the metal trigonal prisms forming isolated infinite zig-zag chains, which are branched by terminal carbon atoms. The way the MBC slabs stack leads to the different structural arrangements. In YBC, they stack in such a way that they face each other, leading to long C···C interslab separations [see Fig. 7(a)]. Similar slabs stack in UBC in such a way that a carbon atom of one slab sits in front of a metal atom of the next slab and conversely [see Fig. 7(b)]. A rotation by 90° of one slab over two in UBC generates the arrangement observed in ThBC, in which the chains are running in two perpendicular directions [see Fig. 7(c)]. Boron chains are regular in YBC and UBC ($d_{B-B}=2.00$ Å and 1.90 Å, and $d_{B-C}=1.64$ Å and 1.52 Å, respectively) [7,8,13]. On the other hand, the boron chains are distorted in ThBC with alternatively short and long B–B bonds ($d_{B-B}=1.77/2.47$ Å and $d_{B-C}=1.54$ Å) [12]. One can even question the existence of a bond for the longest one. In addition to isolated carbon atoms, $Th_3B_2C_3$ contains the same kind of distorted chains ($d_{B-B}=1.77/2.30$ Å) [15]. Values of VEC around 5 are calculated for these kinds of material (see Table 1).

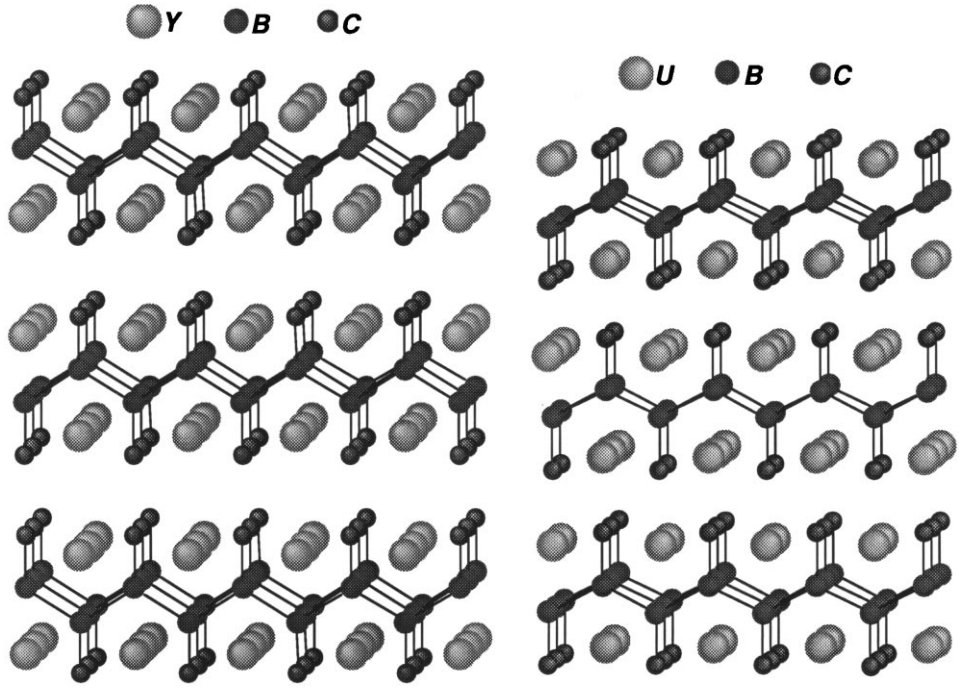

Fig. 7. Structural arrangement of (a) YBC, (b) UBC, and (c) ThBC.

The bonding within a 1-D chain can be nicely understood from the analysis of its band structure [26,27]. This is recalled in Fig. 8(a) for the regular chain. The π MO diagram of the (B_2C_2) unit cell is shown on the left side of the figure. In the extended chain, each of these π levels generates a band. Because of the presence of a screw axis along the regular chain, the bands are degenerate at the edge of the Brillouin zone. Assuming the charge partitioning $(M^{3+})(BC)^{3-}$, the Fermi level lies very close to the bottom of the π_3 band. With (slightly more than) two occupied π bands per B_2C_2 repeat motif, the bonding in the infinite $(BC)^{3-}$ chain can be described by the Lewis formula **10**, which presents two π-electron pairs per B_2C_2 unit. Such a formal electron distribution corresponds to the YBC phase [26,27]. It is interesting to mention that the $(BC)^{3-}$ chain is isoelectronic with a hypothetical polymer of CO, which in fact exhibits a very similar band structure [48]. Indeed, a recent ab initio study on poly-CO suggests that this kind of chain is thermodynamically stable [49]. The potential energy surface associated with the rotation around the C–C single bonds is particularly flat, despite the expectation of some second-order Peierls (i.e. second-order Jahn–Teller) instability arising from the σ/π band crossing near the Fermi level [see Fig. 8(a)]. Therefore, the observed planarity of the 1-D chains in YBC may be imposed by the interaction with the metal atoms [26,27].

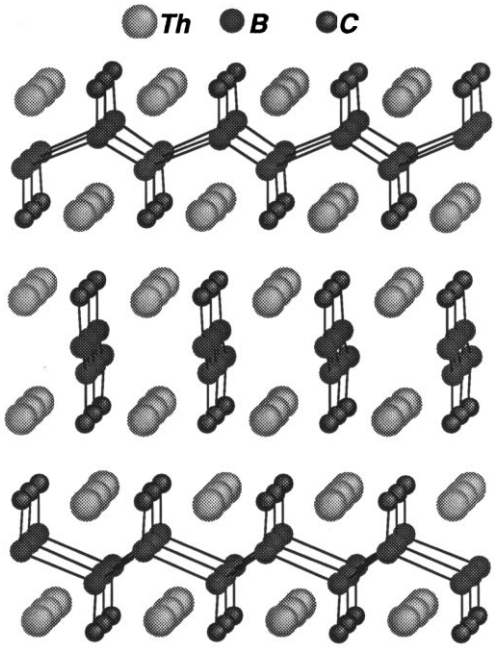

(c)

Fig. 7. (*continued*)

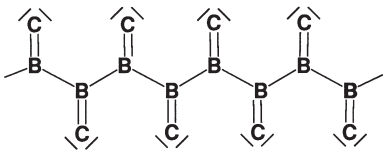

(10)

Going from $(BC)^{3-}$ to $(BC)^{4-}$ corresponds to the full occupation of the π_3 band leading to a HOMO–LUMO degeneracy at the edge of the Brillouin zone [see Fig. 8(a)]. This should induce a Peierls instability which in turn leads to a distorted structure with alternately short and long B–B contacts, opening a band gap at the Fermi level [see Fig. 8(b)] [26,27]. This suggests that the metal is tetravalent in ThBC and $Th_3B_2C_3$ in which distorted chains are present [26,27]. With three occupied π bands per B_2C_2 repeat motif, the bonding in the $(BC)^{4-}$ chain can be described by the Lewis formula **11**, which contains three π-electron pairs per B_2C_2 unit. However, this Lewis formula cannot fully explain the very long B–B contacts observed in the thorium phases [26,27]. Formula **12**, which corresponds to "isolated" $(B_2C_2)^{8-}$ units, can be invoked. However, having different numbers of σ and π electrons than that predicted by the band structure depicted in Fig. 8(b), it cannot be considered as a resonance formula of **11** in a 1-D space. The situation is somewhat

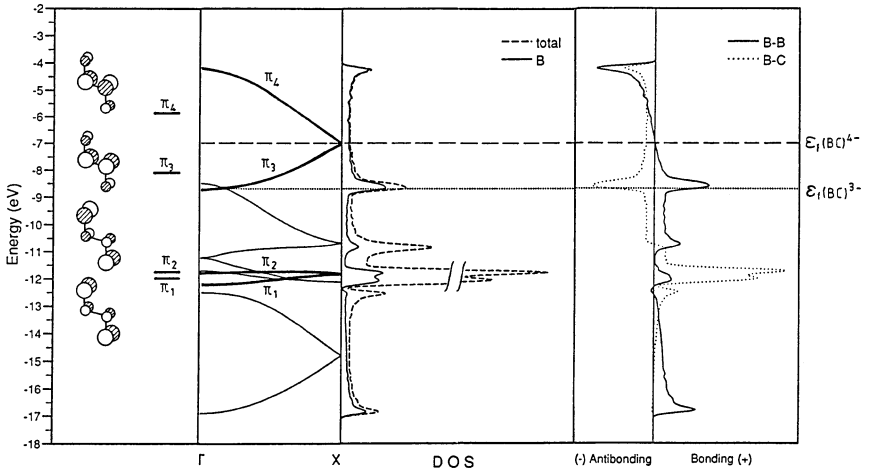

a)

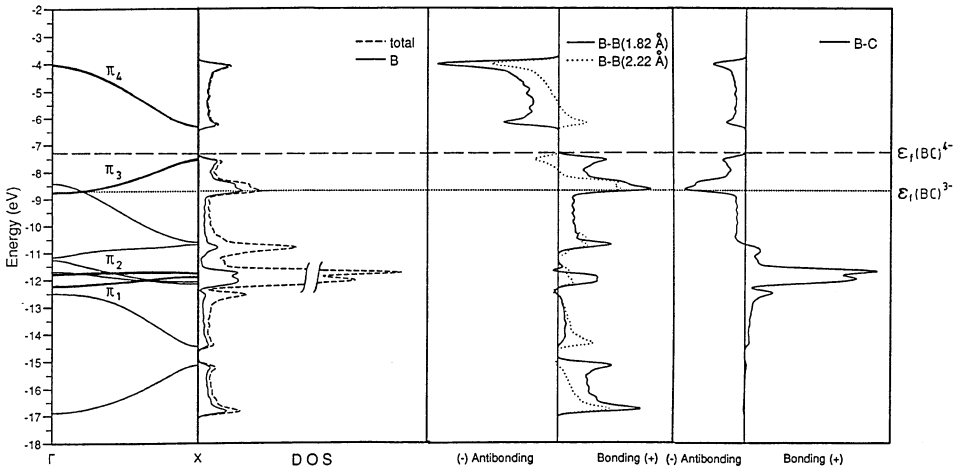

b)

Fig. 8. (a) π MO diagram for the B_2C_2 unit cell, band structure, total density of states (dashed line) with boron contribution (solid line), and COOP curves for B–B (solid line) and B–C (dashed line) contacts for the regular zig-zag $(BC)_\infty$ chain. (b) Band structure, total density of states (dashed line) with boron contribution (solid line), and COOP curves for B–B (solid line) and B–C (dashed line) contacts for the distorted zig-zag $(BC)_\infty$ chain. The Fermi level is indicated for charges of 3− (dotted line) and 4− (dashed line).

different in the full 3-D compound where symmetry allows both configurations to mix. EHTB calculations on ThBC and $Th_3B_2C_3$ indicate that both canonical formulae **11** and **12** have to be considered, the latter having the lowest statistical weight [26,27].

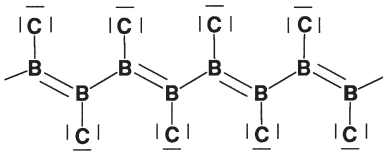

(11)

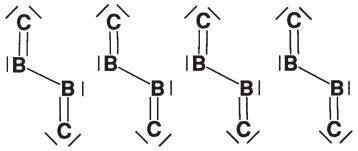

(12)

The various compounds adopting the UBC structural type are slightly more difficult to rationalize, partly because some of the structural data which have been reported are not very accurate. A recent structural determination of UBC indicates regular chains, suggesting the $(U^{3+})(BC)^{3-}$ charge partitioning [26,27]. The boron–carbon chains in the carbon-enriched non-stoichiometric phase $UB_{0.78}C_{1.22}$ are more electron rich [$(U^{3+})(B_{0.78}C_{1.22})^{3-}$ isoelectronic with $(U^{3.22+})(BC)^{3.22-}$] and consequently are expected to be at least slightly distorted, as observed by neutron diffraction ($d_{B-B}=1.71/2.04$ Å) [14], but not by X-ray diffraction ($d_{B-B}=1.89$ Å) [14]. Assuming that the uranium oxidation state is the same in all of these phases (U^{3+}), the $(BN)^{3-}$ chains in UBN are isoelectronic with $(BC)^{4-}$ chains and consequently they should be distorted. Although X-ray powder experiments indicate regular chains ($d_{B-B}=1.89$ Å) [50], it is likely that bond alternation is present in this phase.

Again, as for the MB_2C phases, calculations on the 3-D MBC materials indicate strong covalent character between the metal and non-metal moieties with the Fermi level crossing the bottom of the metallic d band and the top of the B–B bonding band [26,27].

With less electrons per BC unit, higher connectivity is expected as observed in LiBC [51]. According to $(Li^{+})(BC)^{-}$, boron and carbon atoms form 2-D planar layers which are isostructural and isoelectronic with graphite. These graphite-like sheets alternate with hexagonal planes made of alkali metal atoms.

4. Boron–carbon "molecules"

Ternary rare earth metal borocarbide compounds containing finite boron–carbon units encapsulated in metallic channels are more electron-rich than those previously

mentioned, with VEC values spreading over the range 5–6. As shown in Table 1, different kinds of unit have been stabilized in these materials. Two-atom (C_2) and/or three-atom (BC_2) chains are found in metal- and carbon-rich compounds such as Sc_2BC_2 [20], $Ce_5B_2C_6$ [19], and $Gd_5B_2C_5$ [21]. Longer chains are observed when the B/C ratio increases, such as in $La_{15}B_{14}C_{19}$, which contains eleven-membered B_4C_7 and B_5C_6 units [16,28], in $Ce_{10}B_9C_{12}$, in which are inserted 13-membered B_5C_8 chains (the longest thus far observed in these compounds) and eight-membered B_4C_4 chains [17,28], and in $Ce_5B_4C_5$, which contains three-membered BC_2, six-membered B_3C_3 and eight-membered B_4C_4 chains, in addition to single C atoms [18,28]. The B–B, B–C, and C–C bond distances, which vary between 1.57 Å and 1.68 Å, 1.43 Å and 1.58 Å, and 1.30 Å and 1.35 Å, respectively, suggest some double-bond character. The associated bond angles vary from 180° to ca. 140°. The deviation away from linearity of some of these pseudo-molecules probably results from crystal packing forces. The bonding in some of these materials was recently analyzed in detail [28,29].

4.1. A simple example: Sc_2BC_2

In all compounds, the metallic sublattice consists of a three-dimensional (3-D) framework resulting from a regular or irregular stacking of 2-D (sometimes corrugated) square nets. Such an arrangement leads to the formation of small holes of different sizes in which roughly linear B_mC_n units are embedded, as exemplified by Sc_2BC_2 which contains C–B–C entities (see Fig. 9) [20].

The crystal structure of Sc_2BC_2 is related to that of CaC_2. The BC_2 chains are perfectly symmetrical and linear, with B–C distances (1.48 Å) suggesting double bonds. The EHMO diagram of such an isolated unit is shown in Fig. 10. Its level ordering is qualitatively similar to that of CO_2, with a favored valence electron count of 16 leading to a formal charge of 5− [20]. For such an electron count, all the bonding and non-bonding levels are occupied and separated from the empty antibonding orbitals by a large HOMO/LUMO gap. Ab initio calculations at the MP2 level on the 16-electron $(BC_2)^{5-}$ anion located in a modelized cationic environment lead to an optimized distance of 1.49 Å, a value in good agreement with the observed one (1.48 Å) [28,29].

Occupied MOs at relatively high energy and vacant MOs at relatively low energy provide the ingredients for ligands being a good σ-donor, and forming, as in a classical molecular coordination compound, metal–ligand covalent bonding. This was confirmed by EHTB calculations [20]. The analysis of the DOS of Sc_2BC_2 given in Fig. 11 shows that the major bonding interaction occurs via an electron transfer from the occupied bonding and non-bonding orbitals of the $(BC_2)^{5-}$ units into empty states of the metallic d-band. This rather strong metal–ligand covalent character is reflected by the presence of a metallic participation in the boron–carbon valence band and the dispersion of the boron–carbon bands after interaction with the metallic host. The occupation of the BC_2 frontier orbitals in the 3-D solid is consistent with the $(BC_2)^{5-}$ charge assignment, leading to an average formal oxidation state of 2.5+ for the metal atoms. The Fermi level lies at the very bottom of

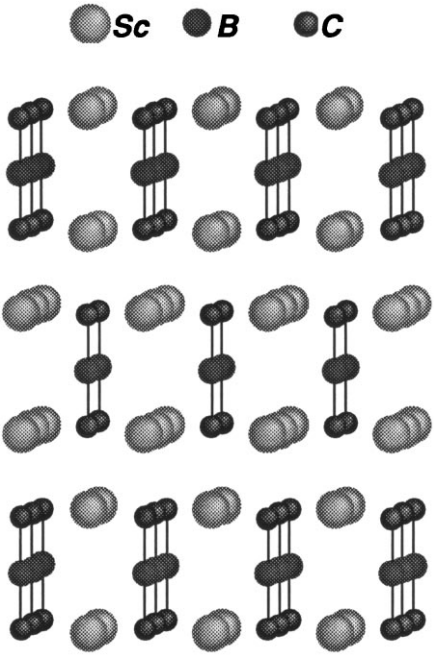

Fig. 9. Structural arrangement of Sc_2BC_2.

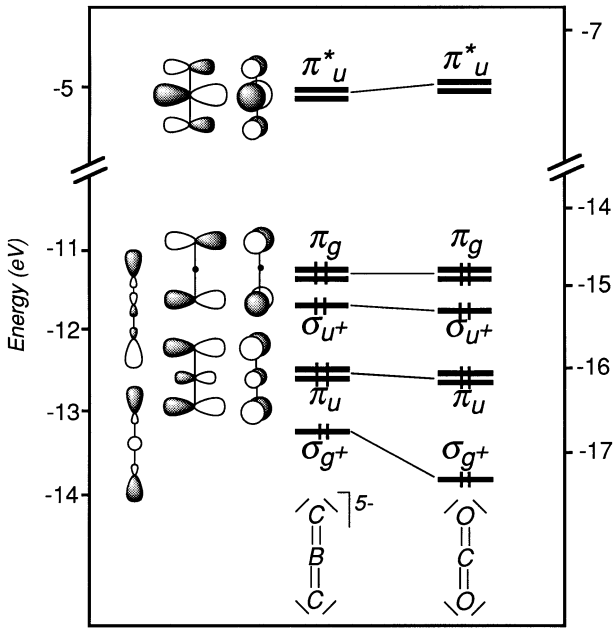

Fig. 10. Comparison of the MO diagrams of $(BC_2)^{5-}$ and CO_2.

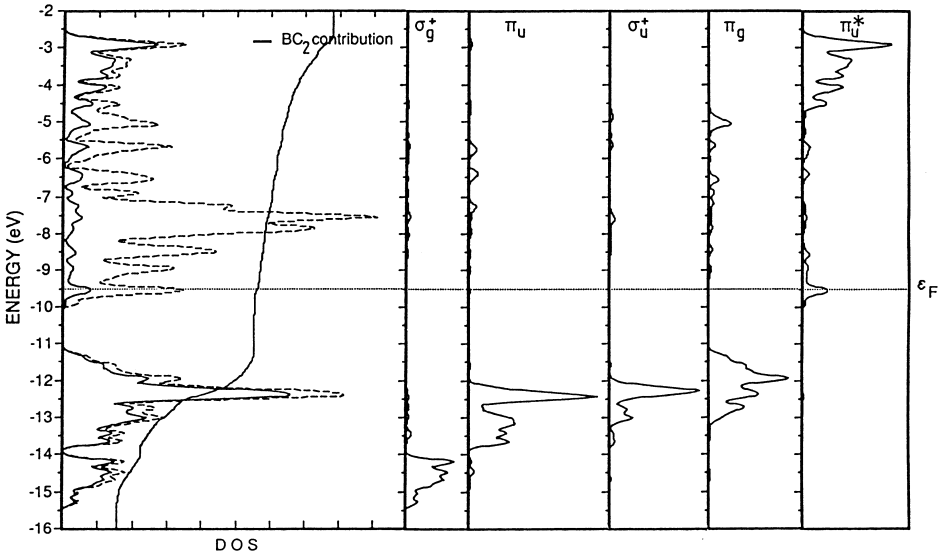

Fig. 11. Total density of states (dashed line), total and FMO contributions of the BC_2 units (solid line) for Sc_2BC_2 (from ref. [20] with permission).

the d-band, in agreement with the fact that there is formally half of an electron per metal atom. Preliminary results obtained from DFT band structure calculations on Sc_2BC_2 support this EHTB analysis [52,53].

4.2. *Other compounds containing triatomic "molecules"*

Other solid-state compounds containing molecular BC_2 units buried in a solid matrix were recently reported. Al_3BC_3, prepared by Hillebrecht and Meyer, contains symmetrical and linear BC_2 chains ($d_{B-C}=1.44$ Å) in addition to isolated carbon atoms [54]. Slightly asymmetrical BC_2 units are found in $Ce_5B_4C_5$ [18], $Ce_5B_2C_6$ [19] and $La_5B_2C_6$ [55]. Preliminary work carried out in our laboratory on $M_5B_2C_5$ (M = Sm, Gd), the structure of which is related to $Ce_5B_2C_6$, indicates that nearly linear BC_2 chains are trapped in metallic holes [21]. Significantly bent BC_2 units are present in the quaternary compounds $La_3Br_2BC_2$ [(C–B–C) = 148°, $d_{B-C}=1.49$ Å] [56] and $La_9Br_5B_3C_6$ [(C–B–C) = 141°, $d_{B-C}=1.51$ Å] [57].

Interestingly, Mattausch et al. describe the bent BC_2 groups in $La_3Br_2BC_2$ and $La_9Br_5B_3C_6$ as 18-electron $(BC_2)^{7-}$ anions, isoelectronic with the bent SO_2 molecule, rather than as 16-electron $(BC_2)^{5-}$ anions [57]. This is supported by DFT calculations [57]. Ab initio calculations at the MP2 level carried out in our laboratory on $(BC_2)^{n-}$ ($n=5$, 6, 7) anions stabilized in a modelized cationic environment led, as expected, to longer B–C separations and smaller bent angles upon the increase of n (1.49 Å and 180° for $n=5$; 1.61 Å and 135° for $n=6$; 1.86 Å and 115° for $n=7$) [28,29]. These results indicate also that a small bending of the BC_2 unit for $n=5$ or forcing the anion to be linear for $n=6$ and 7 are not costly in energy. This suggests

that in all the compounds mentioned above, the BC_2 anionic pseudo-molecules are better described with a formal charge of 5− (or eventually 6− if they are significantly bent) rather than the charge of 7− proposed by Mattausch et al. [28,29]. A comparison can be made with the coordination of CO_2 in transition metal molecular complexes. Examples of coordination modes leading to bent and asymmetrical CO_2-complexed ligands are well documented (see for example ref. [58]). In the solid-state, small constraints of the surrounding metal atoms must be sufficient to allow some weak distortion of the BC_2 chains without modifying too much their electronic structure.

Superconductivity has been reported for $La_5B_2C_6$ ($T_c = 6.9$ K) [59] and $La_9Br_5B_3C_6$ ($T_c = 6$ K) [57]. In both cases metal atoms are not fully oxidized and their electronic band structure exhibits a Fermi level, which cuts rather sharp and important peaks of density of states made of metal and non-metal contributions [28,57]. These compounds present the characteristic "fingerprint" [60] often noticed in the superconducting rare earth metal carbide halides such as $Y_2Br_2C_2$ which contain C_2 groups ($T_c = 3.6$ K) [60–62], or the quaternary intermetallic borocarbides such as $LnNi_2B_2C$ which contain B_2C units [$T_c(\max) = 16.6$ K] ([63–65], for a theoretical study, see refs. [66–69]).

Let us mention that triatomic units isoelectronic with $(BC_2)^{5-}$, such as $(C_3)^{4-}$, $(CBN)^{4-}$, or $(BN_2)^{2-}$, have been trapped in solid-state compounds (see for instance refs. [70,71]). The stability of some of these small anionic species was previously predicted by Pyykö using ab initio results [72].

4.3. Longer chains

Longer "molecular" boron–carbon chains can be observed in other ternary phases such as $Ce_{10}B_9C_{12}$ which contains B_4C_4 and B_5C_8 units (see Fig. 12) [17,28]. It is clear that, for geometrical reasons, the chains cannot be perfectly linear in such a material. Nevertheless, recent results obtained from EHMO and ab initio calculations on the B_mC_n units with their real geometries do not differ much from those obtained for idealized linear structures. The EHMO diagrams of some idealized B_mC_n chains are given in Fig. 13 [28,29]. They indicate that the B_mC_n chains present generally one or two π-type non-bonding levels situated at intermediate energy, in the middle of a large gap separating a set of low-lying orbitals from a set of significantly antibonding orbitals. EHTB calculations on the full 3-D solids find that, in all the rare earth metal borocarbide compounds containing this type of B_mC_n chain, these intermediate levels generate a rather narrow band which partly overlaps the bottom of the metal d-band, and is crossed by the Fermi level. This is illustrated in Fig. 14 for $Ce_{10}B_9C_{12}$ [28]. It follows that these B_mC_n intermediate levels are roughly half-occupied in the solid. This feature is considered favorable for superconductivity (see for instance [73–75]).

From these results, we conclude that the best formal oxidation state which can be ascribed to these pseudo-molecular chains corresponds to a situation in which all the non-bonding orbitals lying at intermediate energy would be the half-occupied HOMO. This leads to the formal charges given at the bottom of Fig. 13. Such

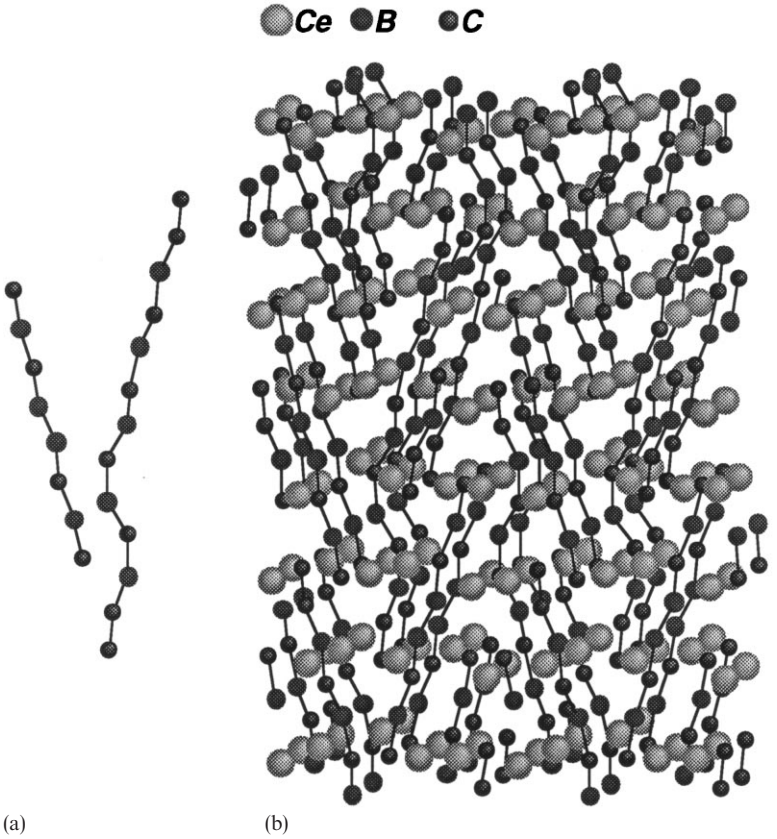

Fig. 12. Structural arrangement of $Ce_{10}B_9C_{12}$: (a) isolated B_4C_4 and B_5C_8 chains; (b) B_4C_4 and B_5C_8 chains in their metallic environment.

formal charges have been confirmed by ab initio calculations on some "isolated" anionic $(B_mC_n)^{x-}$ radicals, which yield optimized bond distances in rather good agreement with the experimental values [28,29].

An intriguing aspect of carbon chemistry is the preparation of infinite linear 1-D rods made of sp-type carbon atoms, called "carbyne" [76,77]. Theoretical studies predict that carbyne will prefer the acetylenic form –(C≡C)– over the cumulenic form =(C=C)= [78]. Assuming the formal charges given in Fig. 13 and discarding their radical nature, the $(B_mC_n)^{x-}$ anions are indeed isoelectronic with hypothetical $(C_n)^{4-}$ cumulenic oligomers, that is pieces of carbyne with the cumulenic-like form which follow the octet rule. From this viewpoint, it appears that the synthesis of a rare earth metal borocarbide material containing very long or even infinite rods of boron and carbon would constitute a good model for the hypothetical metastable allotropic 1-D phase of carbon. With such a charge distribution for the boron–carbon groups, metal atoms in these M–B–C materials are not fully oxidized but roughly

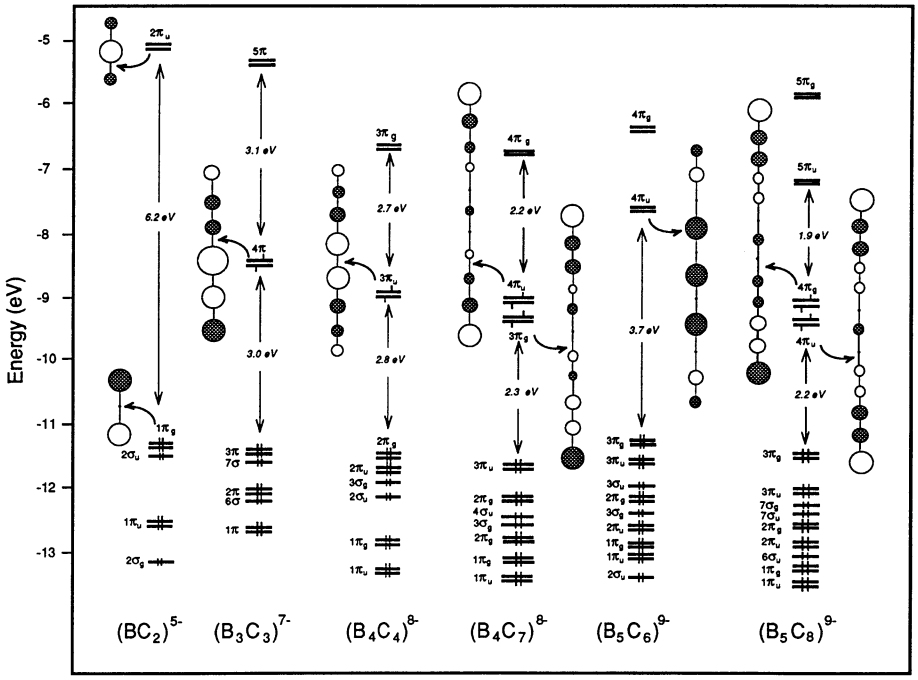

Fig. 13. EHMO diagrams of some isolated $(B_mC_n)^{x-}$ chains (linear models of $C_{\infty v}$ or $D_{\infty h}$ symmetry were assumed) (from ref. [28] with permission).

in the range 2–2.8+ [28,29]. The metal atoms being less oxidized, significant π-backbonding into the π* orbitals of the B_mC_n anions occurs.

5. Covalent metal-to-ligand bonding

It is clear from the discussion above that a simple ionic bonding scheme between metal cations and non-metal anions allows us to rationalize nicely the structure and bonding within the non-metallic framework present in the rare earth metal borocarbides. In most cases, the boron–carbon network can be described with simple Lewis formulae in which the atoms generally satisfy the octet rule. In the case of the extended 2-D or 1-D non-metallic network, the metal is generally fully or almost fully oxidized. In the case of phases containing finite boron–carbon chains, the metal atoms are formally in an oxidation state close to 2+.

Such an approach may bring the reader to the conclusion that metal–ligand covalency is absent from these fascinating materials. Indeed, these substances have a significant degree of metal–ligand covalent bonding, in which the outer electron clouds of the boron–carbon anions are polarized towards the metal cations. Although covalent interaction in these phases is more delocalized in nature, it can be related to the metal–ligand bonding in molecular coordination chemistry. All the calcula-

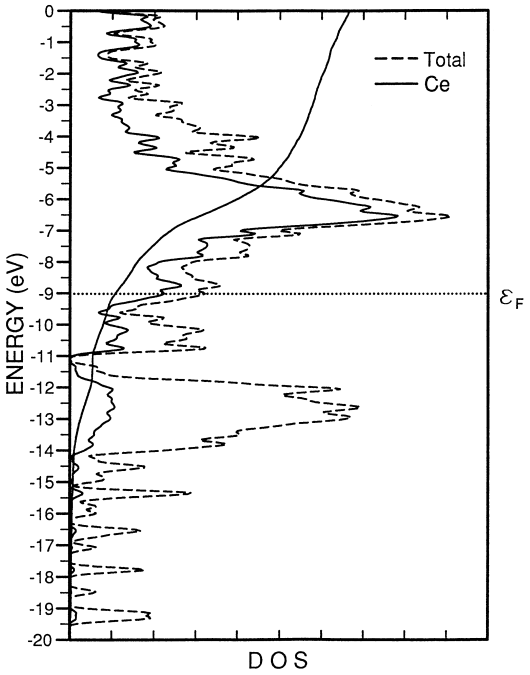

Fig. 14. Total density of states (dashed line) and metallic contribution (solid line) for $Ce_{10}B_9C_{12}$ obtained from EHTB calculations (from ref. [28] with permission).

tions indicate a significant electron transfer from the non-metal anionic system to the metal cations. This metal–ligand interaction is shown in **13**. The highest occupied levels of the non-metallic moiety, which are non-bonding and/or π-bonding, are stabilized by the levels of the d-band, which are empty or largely empty. The metallic levels which participate most in this stabilizing interaction are those of the bottom of the d-band, which are closer in energy to the occupied orbitals of the boron–carbon network. These d levels have metal–metal bonding character. As a consequence, some metal–metal bonding character is conferred on the occupied levels after interaction. This through-bond interaction explains the presence of metal–metal bonding in the phases even when the metal atoms are fully oxidized. In the cases where the metal atoms are not fully oxidized, the occupation of the bottom of the d-band also contributes to metal–metal bonding. Obviously, this metal–metal bonding plays some role in the electron transport properties in these materials (see below), but seems to have no significant effect on the structural arrangement of the non-metal networks. Nevertheless, one should keep in mind that the existence of these various boron–carbon arrangements is due to the presence of the metal atoms which act as stabilizing agents through metal–ligand bonding, as in molecular coordination chemistry.

From both experimental and theoretical data, all these compounds are expected to be metallic conductors. Band overlapping between the two sublattices at the

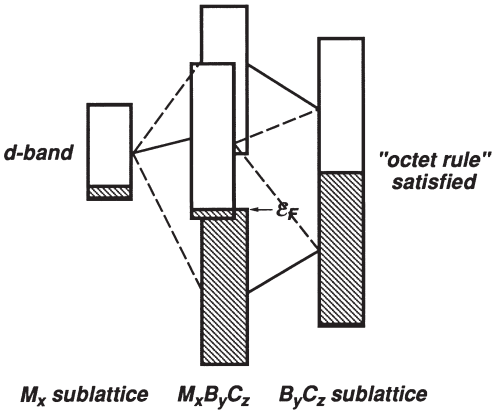

(13)

Fermi level seems to be a common feature of these phases. In the case of compounds containing finite boron–carbon units, the overlapping between the bottom of the metallic d-band and the "intermediate" π-type orbitals of the pseudo-molecular boron–carbon anions yields a narrow peak around the Fermi level with an equal metal/non-metal participation [28,29]. As said previously, such a feature is considered a favorable condition for superconductivity [60], as observed for $La_5B_2C_6$ [59] and the quaternary phase $La_9Br_5B_3C_6$ [57].

6. Conclusion

Although the solid-state language of Zintl–Klemm concept, band structures, and density of states is necessary to rationalize these fascinating compounds, they are governed by the same laws that guide molecular structural chemistry: the relationship between the electron count and the structural arrangement. More precisely, one could think of these materials as solid-state coordination compounds resulting from the complexation of metal cations in a high oxidation state by infinite or finite anionic ligands in which the octet rule is satisfied. This classical bonding mode, i.e. σ-donation, sometimes supplemented by some π-backdonation, can be used to describe these materials. Some of them are particularly closely related to molecular transition metal compounds. Conjugated carbon rods of different length can easily be stabilized when spanned by organometallic caps [79–82]. Close ties between these organometallic species and the solid-state rare earth metal borocarbides containing finite boron–carbon chains are evident. For instance, a $(C_3)^{4-}$ group, isoelectronic with $(BC_2)^{5-}$ contained in Sc_2BC_2, is present in the molecular complex $[\{Re(C_5Me_5)(NO)(PPh_3)Mn(C_5H_5)(CO)_2\}(\mu\text{-}C_3)]^+$ [83]. Study of the bonding in such a species indicates that, as observed in our finite chain-containing borocarbides,

ligand-to-metal electron transfer is rather strong whereas metal-to-ligand backdonation is fairly weak [73–75].

Organometallic chemistry involving 2-D networks of carbon is being investigated. Bunz and coworkers have used metal half-sandwich complexes, along with ethyne and butadiyne units, as building blocks to construct a variety of carbon arrays (see for example ref. [84]). EHTB calculations performed by Burdett and Mortara on such hypothetical arrangements indicate that, unless doped, they are insulating materials with 18-electron metal centers and a carbon array which follows the octet rule [85]. The synthesis of segments of such infinite networks is fairly straightforward, but connecting them into large sheets has been unsuccessful so far. On the other hand, different 2-D organic nets which also follow the octet rule can easily be stabilized in solid-state materials, as exemplified by the MB_2C_2 and MB_2C phases discussed above.

We hope to have impressed on the reader generally interested in molecular transition metal chemistry the fact that the coordination aspect is not restricted to molecular compounds, but can also be encountered in solid-state materials such as the rare earth metal borocarbides discussed in this review. Clearly there is some interest for the molecular chemist in an excursion from time to time into the realms of solid-state chemistry.

Acknowledgements

Thanks are expressed to our coworkers who participated in some of the work mentioned in this review. Drawings of compounds were made based on the X-ray crystallographic data using the Ca.R.Ine Cristallographie 3.0.1 program (C. Boudias and D. Monceau, 1989–1994).

References

[1] N.N. Greenwood, A. Earnshaw, Chemistry of the Elements, Pergamon Press, Oxford, 1984.
[2] G.-Y. Adachi, N. Imakana, Z. Fuzhong, in: K.A. Gschneidner Jr., L. Eyring (Eds.), Handbook on the Physics and Chemistry of Rare Earths, vol. 15, Elsevier, Amsterdam, 1991, p. 62.
[3] A.I. Gusev, Russ. Chem. Rev. 65 (1996) 379.
[4] A.L. Ivanovskii, Russ. Chem. Rev. 66 (1997) 459.
[5] J. Bauer, O. Bars, Acta Crystallogr. B36 (1980) 1540.
[6] G.S. Smith, Q. Johnson, P.C. Nordine, Acta Crystallogr. 19 (1965) 668.
[7] J. Bauer, H. Nowotny, Monatsh. Chem. 102 (1971) 1129.
[8] J. Bauer, J. Less-Common Met. 87 (1982) 45.
[9] P. Rogl, P.J. Fischer, Solid State Chem. 78 (1989) 294.
[10] P. Rogl, P.J. Fischer, Solid State Chem. 90 (1991) 285.
[11] F. Wiitkar, J.-F. Halet, J.-Y. Saillard, P. Rogl, J. Bauer, Inorg. Chem. 33 (1994) 1297.
[12] P. Rogl, J. Nucl. Mater. 73 (1978) 198.
[13] L. Toth, H. Nowotny, F. Benesovsky, E. Rudy, Monatsh. Chem. 92 (1961) 794.
[14] P. Rogl, B. Rupp, I. Felner, P.J. Fisher, Solid State Chem. 104 (1993) 377.
[15] P. Rogl, J. Nucl. Mater. 79 (1979) 154.

[16] P. Gougeon, J.-F. Halet, D. Ansel, J. Bauer, Z. Kristallogr. 211 (1996) 822.
[17] P. Gougeon, J.-F. Halet, D. Ansel, J. Bauer, Z. Kristallogr. 211 (1996) 823.
[18] P. Gougeon, J.-F. Halet, D. Ansel, J. Bauer, Z. Kristallogr. 211 (1996) 824.
[19] J. Bauer, O. Bars, J. Less-Common Met. 83 (1983) 17.
[20] J.-F. Halet, J.-Y. Saillard, J. Bauer, J. Less-Common Met. 158 (1990) 239.
[21] J. Bauer, E. Bidaut, P. Gougeon, J.-F. Halet, R. Pöttgen, unpublished results (1997).
[22] E. Zintl, Angew. Chem. 1 (1939) 52.
[23] W. Klemm, Proc. Chem. Soc. London (1958) 329.
[24] F. Wiitkar, S. Kahlal, J.-F. Halet, J.-Y. Saillard, J. Bauer, P. Rogl, J. Am. Chem. Soc. 116 (1994) 251.
[25] G. Frapper, J.-F. Halet, J.-Y. Saillard, F. Volatron, J. Phys. Chem. 99 (1995) 12164.
[26] F. Wiitkar, S. Kahlal, J.-F. Halet, J.-Y. Saillard, J. Bauer, P. Rogl, Inorg. Chem. 34 (1995) 1248.
[27] L.L. Lohr, Int. J. Quantum Chem. 25 (1991) 121.
[28] D. Ansel, J. Bauer, F. Bonhomme, G. Boucekkine, G. Frapper, P. Gougeon, J.-F. Halet, J.-Y. Saillard, B. Zouchoune, Angew. Chem., Int. Ed. Engl. 35 (1996) 2098.
[29] J. Bauer, G. Boucekkine, G. Frapper, J.-F. Halet, J.-Y. Saillard, B. Zouchoune, J. Solid State Chem. 133 (1997) 190.
[30] R. Hoffmann, J. Chem. Phys. 39 (1963) 1397.
[31] M.-H. Whangbo, R. Hoffmann, R.B. Woodward, Proc. Roy. Soc. London A366 (1979) 23.
[32] M.-H. Whangbo, R. Hoffmann, J. Am. Chem. Soc. 100 (1978) 6093.
[33] E. Canadell, M.-H. Whangbo, Chem. Rev. 91 (1991) 965.
[34] R.G. Parr, W. Yang, Density Functional Theory of Atoms and Molecules, Oxford University Press Oxford, 1989.
[35] W. Kohn, A.D. Becke, R.G. Parr, J. Phys. Chem. 100 (1996) 12974.
[36] E.J. Baerends, O.V. Gritsenko, J. Phys. Chem. A101 (1997) 5384.
[37] R. Pöttgen, unpublished results (1996).
[38] A.T. Balaban, C.C. Rentia, E. Ciupitu, Rev. Roum. Chim. 13 (1968) 231.
[39] A.T. Balaban, C.C. Rentia, E. Ciupitu, Erratum, Rev. Roum. Chim. 13 (1968) 1233.
[40] J.K. Burdett, S. Lee, J. Am. Chem. Soc. 107 (1985) 3063.
[41] J.K. Burdett, E. Canadell, T. Hughbanks, J. Am. Chem. Soc. 108 (1986) 3971.
[42] P.K. Smith, P.W. Gilles, Inorg. Nucl. Chem. 29 (1967) 375.
[43] R. Hoffmann, J. Chem. Soc., Chem. Commun. (1969) 240.
[44] M. Le Floch J. Bauer, J.-F. Halet, J.-Y. Saillard (1997).
[45] M. Wörle, R. Nesper, J. Alloys Comp. 216 (1994) 75.
[46] J. Elguero, C. Foces-Foces, A.L. Llamas-Saiz, Bull. Soc. Chim. Bel. 101 (1992) 795.
[47] R. Gautier, F. Gourves, J.-F. Halet, J.-Y. Saillard, unpublished results (1997).
[48] C.-X. Cui, M. Kertesz, Chem. Phys. Lett. 169 (1990) 445.
[49] G. Frapper, C.-X. Cui, J.-F. Halet, J.-Y. Saillard, M. Kertesz, J. Chem. Soc., Chem. Commun. (1997) 2011.
[50] H. Klesnar, P. Rogl, in: D. Emin (Ed.), AIP Proc. 231 on Boron Rich Solids, Albuquerque, NM, 1991, p. 414.
[51] M. Wörle, R. Nesper, G. Mair, M. Schwarz, H.G. von Schnering, Z. Anorg. Allg. Chem. 621 (1995) 1153.
[52] R. Gautier, J.-F. Halet, J.-Y. Saillard, unpublished results (1998).
[53] A.C. Switendick, 10th Int. Conf. on Solid State Compounds of Transition Elements, Münster, Germany, 21–25 March 1991.
[54] H. Hillebrecht, F.D. Meyer, Angew. Chem., Int. Ed. Engl. 35 (1996) 2499.
[55] J. Bauer, O. Bars, J. Less-Common Met. 95 (1983) 267.
[56] Hj. Mattausch, A. Simon, Angew. Chem., Int. Ed. Engl. 34 (1995) 1633.
[57] Hj. Mattausch, A. Simon, C. Felser, R. Dronskowski, Angew. Chem. Int. Ed. Engl. 35 (1996) 1685.
[58] C. Mealli, R. Hoffmann, A. Stockis, Inorg. Chem. 23 (1984) 56.
[59] J. Bauer, C. Politis, J. Less-Common Met. 88 (1982) L1.
[60] A. Simon, Angew. Chem., Int. Ed. Engl. 36 (1997) 1788 and references cited therein.
[61] U. Schwanitz-Schüller, A. Simon, Z. Naturforsch. B40 (1985) 710.

[62] A. Simon, Hj. Mattausch, G.J. Miller, W. Bauhofer, in: K.A. Gschneidner Jr., L. Eyring (Eds.), Handbook on the Physics and Chemistry of Rare Earths, vol. 15, Elsevier, Amsterdam, 1991, p. 191.
[63] R. Nagarajan, C. Mazumdar, Z. Hossain, S.K. Dhar, K.V. Gopalakrishnan, L.C. Gupta, C. Godart, B.D. Padalia, R. Vijayaraghavan, Phys. Rev. Lett. 72 (1994) 274.
[64] R.J. Cava, H. Takagi, H.W. Zandbergen, J.J. Krajewski, W.F. Peck Jr.,, W.T. Siegrist, B. Batlogg, R.B. van Dover, R.J. Felder, K. Mizuhashi, J.O. Lee, H. Elsaki, S. Uchida, Nature 367 (1994) 252.
[65] T. Siegrist, H.W. Zandbergen, R.J. Cava, J.J. Krajewski, W.F. Peck Jr., Nature 367 (1994) 254.
[66] J.K. Burdett, S. Sevov, Inorg. Chem. 33 (1994) 3857.
[67] J.-F. Halet, Inorg. Chem. 33 (1994) 4173.
[68] G. Miller, J. Am. Chem. Soc. 116 (1994) 6332.
[69] G. Miller, in: S.T. Oyama (Ed.), The Chemistry of Transition Metal Carbides and Nitrides, Blackie Academic and Professional, London, 1996, p. 134.
[70] R. Pöttgen, W. Jeitschko, Inorg. Chem. 30 (1991) 427.
[71] H.-J. Meyer, R. Hoffmann, Z. Anorg. Allg. Chem. 607 (1992) 57 and references cited therein.
[72] P. Pyykkö, Y. Zhao, J. Phys. Chem. 94 (1990) 7753.
[73] D.L. Lichtenberger, S.K. Renshaw, Organometallics 12 (1993) 3522.
[74] F. Frapper, M. Kertesz, Inorg. Chem. 32 (1993) 732.
[75] M.I. Bruce, P. Low, K. Costuas, J.-F. Halet, unpublished results (1998).
[76] F. Diederich, Y. Rubin, Angew. Chem., Int. Ed. Engl. 31 (1992) 1101.
[77] F. Diederich, Nature 369 (1994) 199 and references cited therein
[78] M.J. Rice, A.R. Bishop, D.K. Campbell, Phys. Rev. Lett. 51 (1983) 2136.
[79] U.H.F. Bunz, Angew. Chem., Int. Ed. Engl. 35 (1996) 969.
[80] M. Brady, W. Weng, Y. Zhou, J.W. Seyler, A.J. Amoroso, A.M. Arif, M. Böhme, G. Frenking, J.A. Gladysz, J. Am. Chem. Soc. 119 (1997) 775.
[81] M.I. Bruce, Coord. Chem. Rev., 166 (1997) 91.
[82] C. Lapinte, F. Paul, Coord. Chem. Rev. 178–180 (1998) 429–507.
[83] W. Weng, J.A. Ramsden, A.M. Arif, J.A. Gladysz, J. Am. Chem. Soc. 115 (1993) 3824.
[84] U.H.F. Bunz, Chem. Ber. 129 (1996) 785 and references cited therein.
[85] J.K. Burdett, A.K. Mortara, Chem. Mater. 9 (1997) 812.